



DEGRADATION OF DYE BY TiO₂ NANOPARTICLES

Kanjur Wangdi,
 National Food Testing Lab,
 Bhutan Agriculture and Food Regulatory Authority,
 Thimphu, Bhutan

Abstract- Present work shows the comparative study of bare and metal loaded TiO₂ nanoparticles of different phase (anatase and rutile) for the photodegradation of methylene blue dye under visible light irradiation. Anatase TiO₂ nanoparticles were prepared by sol gel method and rutile TiO₂ nanoparticles were prepared by calcining P25- TiO₂ at 800 °C for 2 hours in a muffle furnace. Different weight percent (0.2- 1 wt%) of silver metal were loaded over the prepared TiO₂ catalyst by wet impregnation-reduction method. The Photodegradation of methylene blue dye (20 mL, 0.01 mM) was carried out by using TiO₂ nanoparticles (20 mg) and metal loaded TiO₂ nanoparticles under visible light irradiation. Bare anatase TiO₂ was found to be inactive for the photodegradation of dye under the visible light. However, silver loaded anatase TiO₂ nanoparticles degraded methylene blue dye under the visible light efficiently. 0.5 wt% silver loaded anatase TiO₂ degraded the dye within 45 minutes. Bare rutile TiO₂ also found to be almost inactive for methylene blue degradation under visible light irradiation. However, 0.5 wt% silver loaded rutile TiO₂ degraded the dye within 25 minutes. Interestingly 0.5 wt% silver loaded rutile degraded the dye in just 5 minutes under sunlight irradiation. The results show that the silver metal loaded rutile TiO₂ nanoparticles are more active for the dye degradation under visible light irradiation as compared to their anatase counterparts.

Keywords—Metal Loaded Nanoparticles, Dye Degradation, Photo-degradation, Photo-oxidation

I. INTRODUCTION

In the recent year lots of research has been carried out to use the semiconductor nanoparticles in the various chemical and physical processes, amongst which TiO₂ gained much attention due to its chemical inertness, low cost, non-toxicity, easy availability and it shows excellent photocatalytic activity in the field of environmental applications. The mechanism of TiO₂ involves the generation of electrons (e⁻) in the TiO₂ conduction band and the positive holes (h⁺) the in valence band upon photoirradiation with light energy greater than or

equal to its band gap energy. The photoexcited electrons (e⁻) induce reduction and the positive holes (h⁺) can carry out oxidation of the chemical substances adsorbed [1-5] on the surface of the photocatalyst and convert the photonic energy into chemical energy.

In nature TiO₂ exist in three common polymorphs namely rutile, anatase and brookite. Anatase is having energy difference to that of rutile (~2 to 10 kJ/mol). Rutile polymorph is stable and the other two are the metastable forms which can be converted to the rutile form at higher temperature [6]. Rutile has a body-centred tetragonal unit cell, with unit cell parameters a=b=4.584 Å, and c=2.953 Å. The band gap energy of rutile is E_g=3.00 eV which play an important role in the photocatalytic processes. More over rutile has the highest refractive indices, birefringence and dispersion properties owing to which it is used in the manufacture of optical elements. The third polymorph of TiO₂ is brookite whose structure is built up of distorted octahedral is of less importance for all the processes discussed above because it is unstable [7-8]

Sl. no	Properties	Rutile	Anatase	Brookite
1	Crystal structure	Tetragonal	tetragonal	orthorhombic
2	Band gap energy	3.00eV	3.13eV	3.21eV
3	Lattice constant(Å)	a = 4.5936 c = 2.9587	a = 3.784 c = 9.515	a = 9.184 b = 5.447 c = 5.154
4	Density (g cm ⁻³)	4.13	3.79	3.99



5	O-Ti-O bond angle	81.2°-90.0°	77.7° - 92.6°	77.0°-105°
7	Volume/ molecule (Å ³)	31.2160	34.061	32.172

Table 1: Comparison amongst different polymorphs of TiO₂

Among all the three polymorphs of TiO₂, anatase structure is preferred over other polymorphs for environmental processes such as deodorization, water purification, air purification, sterilization, solar cell applications and photocatalysis reactions because of its higher electron mobility, low dielectric constant and lower density. However, recently rutile TiO₂ has been found to be more selective for photocatalytic oxidation. It has been found that rutile titania is more selective for the oxidation of benzyl alcohol and 4-methoxy benzyl alcohol into corresponding aldehydes [9-12] and the experiment pointed the primary influence of crystallinity of rutile titania on the selectivity.

The photocatalytic activity of TiO₂ can be further improved by metal loading. The role of loaded metal is trapping and subsequent transfer of photoexcited electron onto photocatalyst surface and decreasing the recombination of hole-electron pairs. It is reported that monocrystalline TiO₂ codoped with optimal concentrations of Eu³⁺ and Fe³⁺ (1% Fe³⁺ and 0.5% Eu³⁺) showed significantly enhanced photocatalytic activity compared to undoped TiO₂. Fe³⁺ serves as a hole trap and Eu³⁺ as an electron trap, increasing the rates of anodic and cathodic processes *via* improved interfacial charge transfer. [13]. (Cu, N)-codoped TiO₂ nanoparticles was prepared and investigated the influence of the amounts of Cu and N codoped into TiO₂ on the photocatalytic activity. Codoping of TiO₂ with N and Cu extended absorption upto 590 nm and gave higher photocatalytic activity than pure N- or Cu-doped TiO₂ for the photocatalytic degradation of xylenol orange, thus revealing a potential application in degrading organic pollutants.[14]

A. DYE DEGRADATION

The increase of population culminated the development of different industries to fulfil the needs of human kind. In many ways there is so much of negative environmental impacts by different industries amongst which the textile industry contributes at large. A total of 15% of the total world production of dyes is lost during the dyeing process and is released in textile effluents [15]. Textile dyes in wastewater are a concern not only because they are displeasing aesthetically but are linked to health hazards as well. It is therefore our responsibility to come up with different

techniques to tackle the problem. The dye degradation process by TiO₂ nanoparticle gained lots of interest because of its low cost, low toxicity, and easy availability.

Amongst different purification processes, oxidative process is more promising because of destruction of chromophores thereby removing the color which is main undesirable factor for the water recycling. Photocatalyst, titania (TiO₂) has so far been shown to be the most promising material used for both fundamental research and practical applications because of its high activity, good chemical inertness, safeness, nontoxicity, and low cost. However, pure TiO₂ is only active under ultraviolet (UV) light irradiation (E_g = 3.2 eV), limiting its practical application in the visible region. Activation of TiO₂ is achieved through the absorption of radiation of ultra band gap energy, resulting in the promotion of electrons from the valence band to the conduction band. This will create holes in the valence band. The holes can scavenge H₂O and OH molecules on the surface of the nanoparticle to form OH• radicals. The OH• radicals are highly oxidizing, attacking any organic compounds adsorbed onto the particle surface to form water and carbon dioxide. Electron hole recombination is major competitive deactivation process for this oxidation reaction [16]. During the advanced oxidation process the generation of OH• radicals are considered to be the main oxidative species in UV/TiO₂ process:

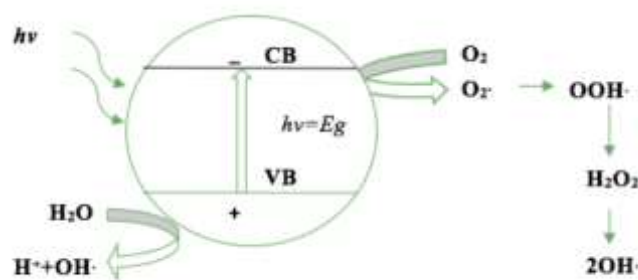
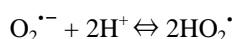
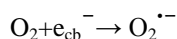
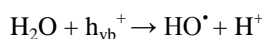


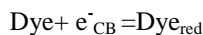
Fig. 1. Generation of oxidative OH radical on TiO₂ surface.



The increase in the amount of catalyst increased the number of active sites on the photocatalytic surface, which in turn,

increased the number of hydroxyl and superoxide radicals, enhancing the photocatalytic activity.

During the dye degradation processes:



II. EXPERIMENTAL

A. MATERIALS

Titanium tetrachloride (TiCl_4), Sodium Borohydride (NaBH_4), Silver Nitrate (AgNO_3), Methylene blue dye (MB) and Degussa P-25 were purchased from the Image Chemicals and they were used without further purification. The deionized water was obtained from the Material Research Lab, Sharda University.

B. PREPARATION OF ANATASE TiO_2

The Anatase phase Titanium Dioxide nanoparticle (TiO_2) was prepared using the sol-gel method [17]. Briefly 14 mL of Titanium Tetrachloride (99.9%) was added into the 140 mL absolute ethyl alcohol (99.9%). The reaction was carried out with the continuous stirring in the fume hood due to the generation of Cl_2 and HCl gases at room temperature. The resulting yellow solution was allowed to rest and cool at room temperature as the gases evolved ceased. The obtained suspension was then dried at 80°C in the oven for 12 h. Then it is crushed into a fine powder using a mortar and pestle and the powder.

C. PREPARATION OF CRYSTALLINE TiO_2

Further above prepared TiO_2 was calcined at 800°C for two hours and named as $\text{TiO}_{2\text{cryst}}$. when it is calcined, it yielded the Anatase phase TiO_2 but with the increased crystallinity.

D. PREPARATION OF RUTILE TiO_2

1 g of commercially available Degussa P-25 was taken in the silica crucible and calcined at 800°C in the muffle furnace for 2 h. After the thermal treatment, the powders were cooled down at room temperature and are stored in the moisture free containers and named as R- TiO_2 .

E. METAL LOADING OVER TiO_2 , $\text{TiO}_{2\text{cryst}}$ AND R- TiO_2

Different weight percentages of metal(Ag) were loaded over the TiO_2 , $\text{TiO}_{2\text{cryst}}$ and R- TiO_2 via wet impregnation-reduction methods (Ag/TiO_2 , $\text{Ag}/\text{TiO}_{2\text{cryst}}$ and $\text{Ag}/\text{R-TiO}_2$), as there are

regular dispersion of smaller metal particles and agglomeration doesn't occur unlike photodeposition methods [18-19]. For the 1 wt%, 100 mg each of the catalysts were taken in the 100 mL beaker. Into the beaker, 5mL deionized water was added. Then 935 μL of 0.01 M AgNO_3 was added. Under the constant stirring condition, 10 μL of Sodium borohydride (NaBH_4) was added until the solution became brownish. Then it was constantly stirred for 48 h after which it was washed with deionized water for several times. Finally, it was rinsed with methanol or acetone and are dried in an oven at 50°C until it became completely dry. The metal loaded samples displayed different color depending on the weight % of the metal loaded (Fig. 1). Then the metal loaded phases were obtained and stored in moisture free vials. In the same manner 0.2 wt %, 0.5 wt% were loaded on respective samples for the comparative studies.

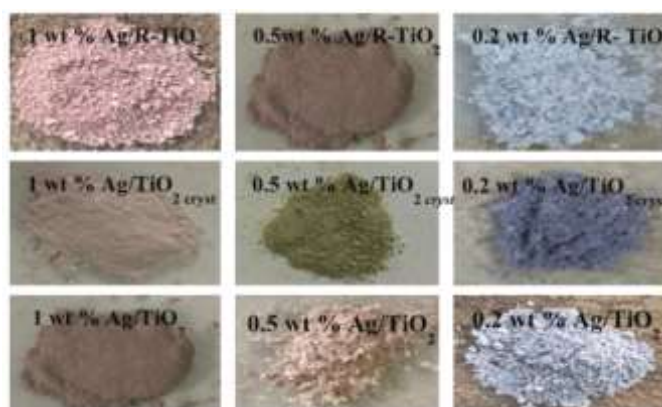


Fig. 2. Colors displayed by different catalysts upon metal loading.

F. CHARACTERIZATION TECHNIQUES

The absorbance of TiO_2 , $\text{TiO}_{2\text{cryst}}$ and R- TiO_2 were confirmed using UV-Visible Spectrophotometer (UV 1800) by Shimadzu Corporation. The wavelength of operation was 200 nm-800 nm. Infrared Spectrometer (Cary 630 FTIR) by Agilent was used to confirm the presence of functional group and nature of bonding. The presence of the different phases of TiO_2 and the particle size were confirmed by the X-Ray Diffractometer (Ultima IV) by Rigaku. The $\text{K}\beta$ filter, radiation operated at 40 kV, 40 mV and the scan speed/time 2° per minute.

G. DEGRADATION OF MB BY METAL LOADED TiO_2

The photodegradation of MB was carried out comparatively for Bare TiO_2 , $\text{TiO}_{2\text{cryst}}$, R- TiO_2 and different wt% metal loaded catalysts. For each, 200mg of catalyst and 20 mL of 0.01mM MB were taken in the 100 mL beaker. For the first 20

mins the dye solution in the presence of catalyst was continuously stirred in the dark room to allow the adsorption of dyes on the catalyst surface and eventually reach the adsorption-desorption equilibrium [20]. Then visible light source (LED bulb, 17watt) was switched on to enhance the photodegradation processes and the degradation process was repeated at different time intervals. It was then centrifuged at 9000rpm for 3 minutes and the solution was analyzed using the UV-Spectrophotometer. The visible reactor for the photodegradation process is as shown below;

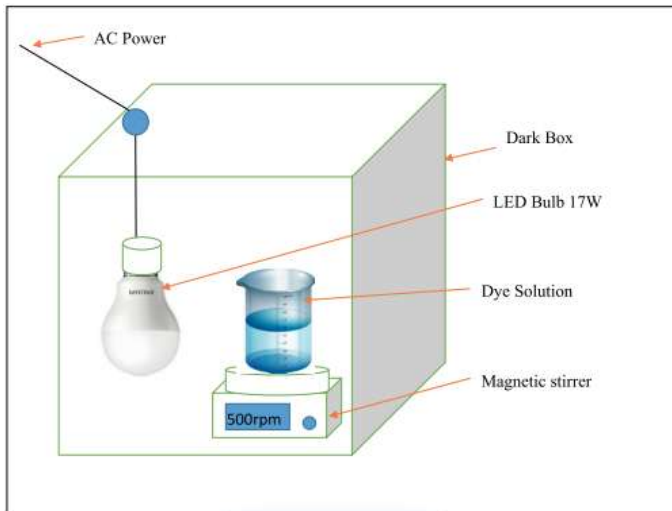


Fig. 3. Visible Reactor set up for Photodegradation process

III. RESULTS AND DISCUSSION

A. CHARACTERIZATION OF CATALYST

The UV absorption spectra of TiO_2 showed onset at around 380 nm which corresponds to anatase phase as shown in Fig. 4. The UV absorption spectra of $\text{TiO}_2_{\text{cryst}}$ shows a red shift in the spectra and its onset comes around 390 nm which is an indication of the conversion of some anatase phase into some rutile phase.

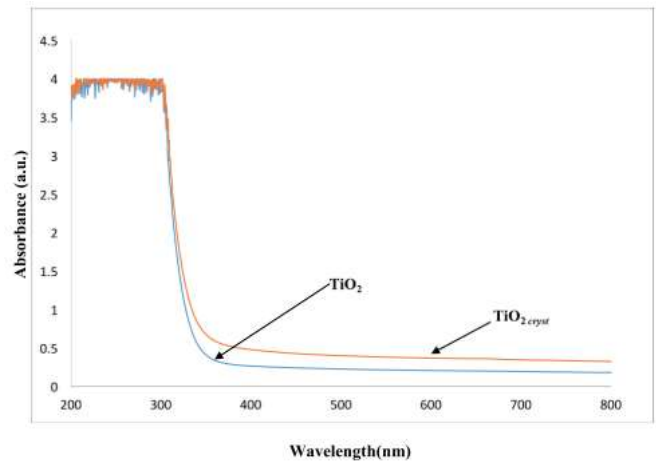


Fig. 4. Absorption spectra of TiO_2 and $\text{TiO}_2_{\text{cryst}}$

FTIR results of the TiO_2 , $\text{TiO}_2_{\text{cryst}}$, R- TiO_2 and Ag/R- TiO_2 showed an intense peak at around 520 cm^{-1} that corresponds to the Ti-O bond (Fig. 5). In the TiO_2 sample there was broad and intense peak at around 3400 cm^{-1} and 3600 cm^{-1} which is attributed to the presence of OH group. The peaks that correspond to the OH group gradually disappeared when its calcined at $400\text{ }^\circ\text{C}$ and for the R- TiO_2 there was a complete absence. It was found that the metal loading over R- TiO_2 showed no effect.

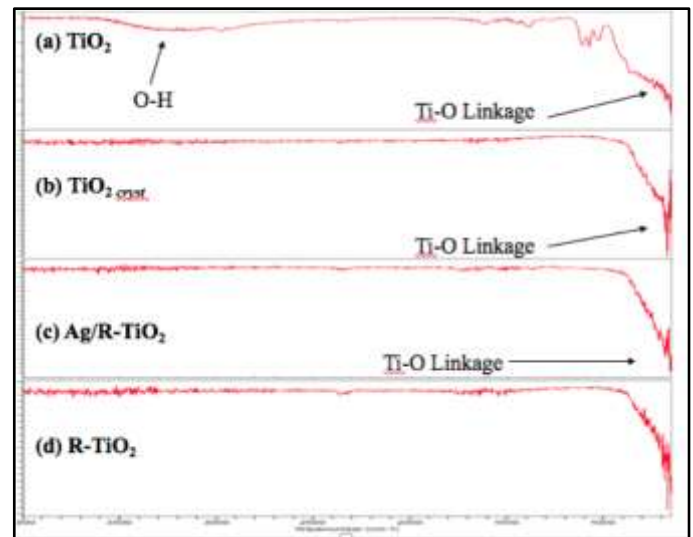


Fig. 5. Infrared Spectra of (a) TiO_2 , (b) $\text{TiO}_2_{\text{cryst}}$ (c) Ag/R- TiO_2 , (d) R- TiO_2

XRD pattern of TiO_2 showed strong diffraction peaks at 25.2° , 37.8° , 47.9° , 54.0° and 62.6° (Fig. 6a) that corresponds to the standard peaks of Anatase phase TiO_2 . Further in (Fig. 6b) $\text{TiO}_2_{\text{cryst}}$ XRD spectra shows highly intense peaks due to the increased crystallinity of TiO_2 after calcination at $400\text{ }^\circ\text{C}$.

Also, in addition to the characteristic peak of anatase TiO_2 at 25.2° , there is an introduction of rutile phase indicated by a small peak present at 27° (Fig. 6d). XRD spectra of 1wt % silver loaded TiO_2 is as indicated in Fig. 6c. When the silver is loaded over the TiO_2 , Ag_2O phase was also found alongside the spectrum of the TiO_2 .

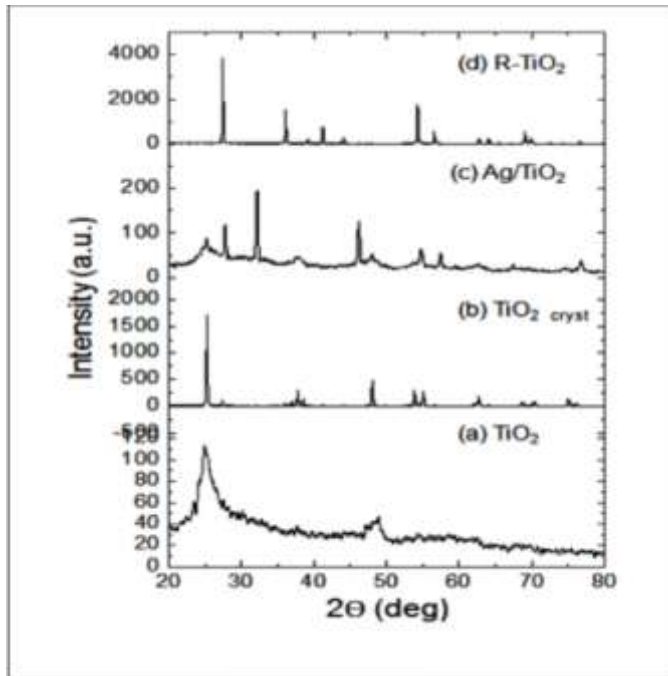


Fig. 6. XRD pattern for (a) TiO_2 (b) $\text{TiO}_{2\text{cryst}}$ (c) Ag/TiO_2 (d) R-TiO_2 .

B. DEGRADATION OF MB BY SILVER LOADED TiO_2 , $\text{TiO}_{2\text{cryst}}$ and R-TiO_2 .

All the catalysts namely TiO_2 , $\text{TiO}_{2\text{cryst}}$ and R-TiO_2 in their bare as well as metal loaded, were found to be inactive in the absence of light. This can be seen from the (Fig.7). The reason for its inactivity is due to no photo-excitation of electrons from the valence band to the conduction band and eventually no free radicals are generated. There is only adsorption-desorption phenomenon and its equilibrium is maintained.

The Photodegradation of MB with bare TiO_2 , Bare R-TiO_2 and Bare $\text{TiO}_{2\text{cryst}}$ was found to be very negligible even if the time of degradation was increased up to an hour (Fig. 10). It can be accounted due to the large band gap energy (3.2 eV) of the TiO_2 nanoparticles limiting its activity under the visible light but needs to be irradiated by the high energy UV light.

The reason for loading metal over the titania was to shift the absorption edge in the visible region and to decrease the electron-hole recombination rate eventually increasing the quantum yield [21]. By doping any impurities over the titania

increases the valence band edge thus lowering the band gap without lowering the conduction band [22].

The photodegradation rate was found increase drastically when the different percentages of silver metals were loaded upon TiO_2 , R-TiO_2 and $\text{TiO}_{2\text{cryst}}$. The increased rate of dye degradation may be attributed to the Ag effectively capturing the photoinduced electrons. The metal particles act as a sink for the photogenerated electrons reducing the rate of their combination with the holes [23].

Before the photodegradation of dyes using TiO_2 nanoparticles the MB dyes were first allowed to get adsorbed over the catalysts. For this purpose, the dye was stirred at 500 rpm in the presence of catalyst in the dark. Fig. 8a shows the dark adsorption of $\text{TiO}_{2\text{cryst}}$. It clearly shows the dyes getting adsorbed over the catalyst in within 60 minutes which on further stirring the desorption process happens.

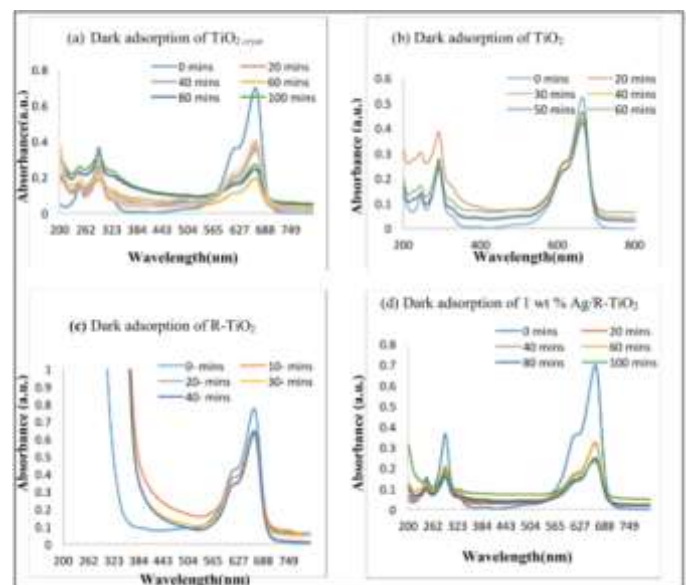


Fig. 7. Dark absorption of (a) $\text{TiO}_{2\text{cryst}}$ (b) TiO_2 (c) R-TiO_2 and (d) 1 wt% $\text{Ag}/\text{R-TiO}_2$.

(Fig. 8) shows the degradation of MB by 1 wt % Ag/TiO_2 . It was found that within 45 minutes of irradiation of visible light, the dye almost degraded but not completely yet. Fig. 8b shows the degradation of dye by 0.5 wt % Ag/TiO_2 which showed that even after 60 minutes of the irradiation of visible light there is only a negligible amount of dye degraded. Further Fig. 9c shows the degradation of MB by 0.2 wt % Ag/TiO_2 which showed even more negligible degradation compared to the previous catalyst. Having loaded different percentages of silver over TiO_2 , 1 wt % Ag/TiO_2 was found to be the better catalysts for the dye degradation compared to the other two.

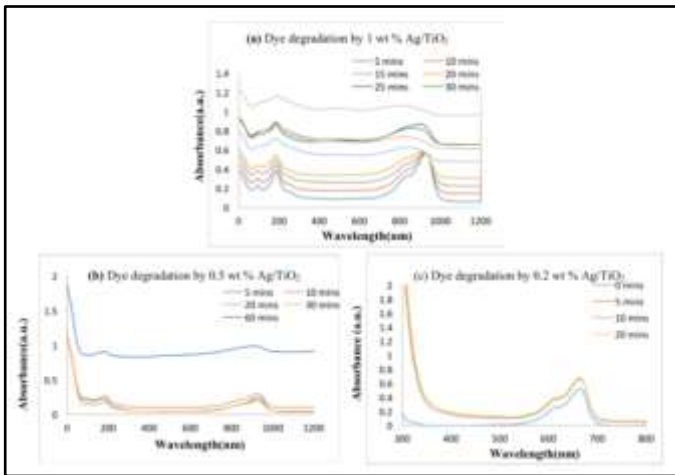


Fig. 8. Dye degradation by (a) 1 wt % Ag/TiO₂, (b) 0.5 wt % Ag/TiO₂ and (c) 0.2 wt % Ag/TiO₂.

Fig. 10a shows the degradation of MB by the 1 wt % Ag/TiO_{2cryst}. Within 30 minutes of irradiation under the visible light the dye was found to degrade to a large extent but not completely. But within 25 minutes of irradiation of visible light in the presence of 0.5 wt % Ag/TiO_{2cryst} (Fig. 10b) the dye was found to degrade completely. Again when 0.2 wt % Ag/TiO_{2cryst} (Fig. 10c) was used as a catalyst, there was only negligible degradation at 25 minutes of irradiation.

Fig. 11a shows the degradation of MB by the 1 wt % Ag/R-TiO₂. After the irradiation time of 20 minutes the dye almost degraded completely but the same concentration of dye was found to be degraded completely around 20 minutes by 0.5 wt % Ag/TiO₂ (Figure 11b). Further when the rate of degradation was compared to that of 0.2 wt % Ag/R-TiO₂, Fig. 11c there was only negligible degradation at the same period of time.

The above observations could be attributed to the dosage level as it plays as an important role in the enhancement of the effect of the noble metal. Below an optimum level, the loaded metal acts as an electron-hole separation centers which improve the charge separation and increase the efficiency of the modified TiO₂ but in contrast when the dosage level exceeds the optimum level the loaded metal acts as an electron hole recombination centers as well as shades the photosensitive surface of TiO₂ [24].

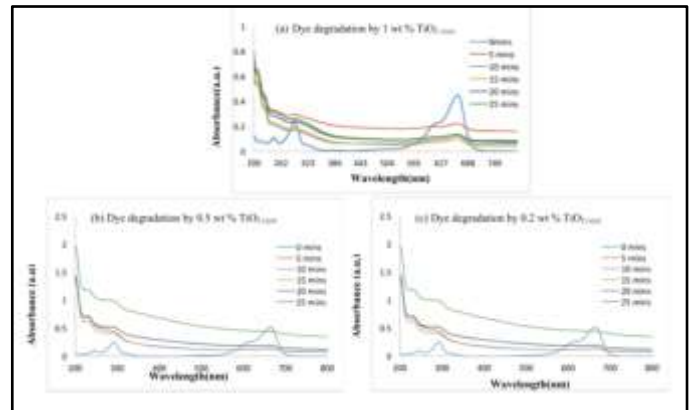


Fig. 9. Dye Degradation by (a) 1 wt % Ag/TiO_{2cryst}, (b) 0.5 wt % Ag/TiO_{2cryst} and (c) 0.2 wt % Ag/TiO_{2cryst}.

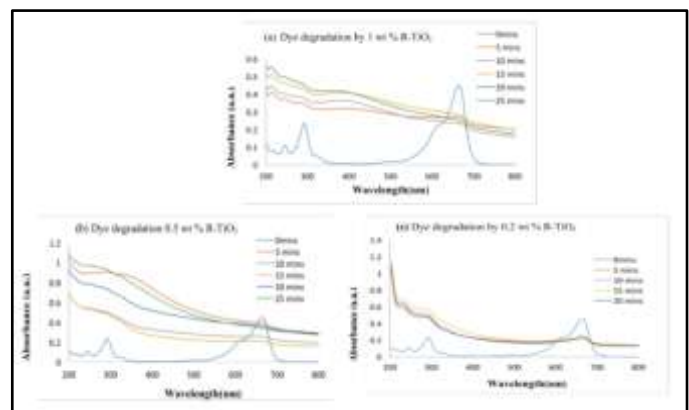


Fig. 10. Dye Degradation by (a) 1 wt % Ag/R-TiO₂, (b) 0.5 wt % Ag/R-TiO₂ (b) and (c) 0.2 wt % Ag/R-TiO₂.

C. DEGRADATION OF DYE IN SUNLIGHT

The degradation of dye was also carried out not only in the Visible light irradiation but also in the sunlight. Surprisingly the rate of degradation of dye drastically increased Fig. 11. Figure 11a shows the degradation MB by 0.5 wt % Ag/TiO_{2cryst}. Interestingly, it was found that the complete dye degradation happened in just 5- 10 minutes which otherwise took around 25 minutes to degrade the same concentration of dye in visible light irradiation. Even 1 wt % Ag/TiO₂ (Fig. 14b) took just 25 minutes to completely degrade the dye which took more than 45 minutes to degrade the dye under visible light irradiation. The improved photocatalytic activity could be attributed to the increase of the intensity of light under which the photodegradation is carried out.

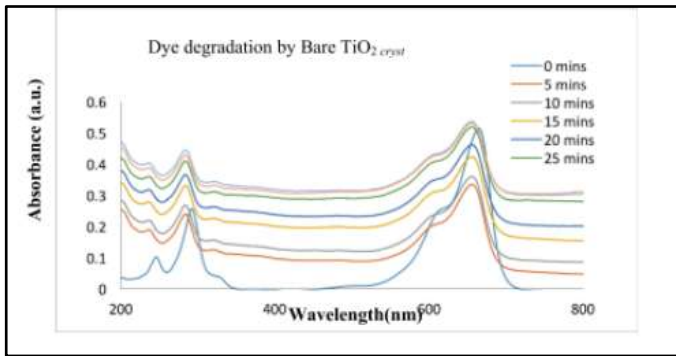


Fig. 10. Dye Degradation by Bare TiO_{2cryst}

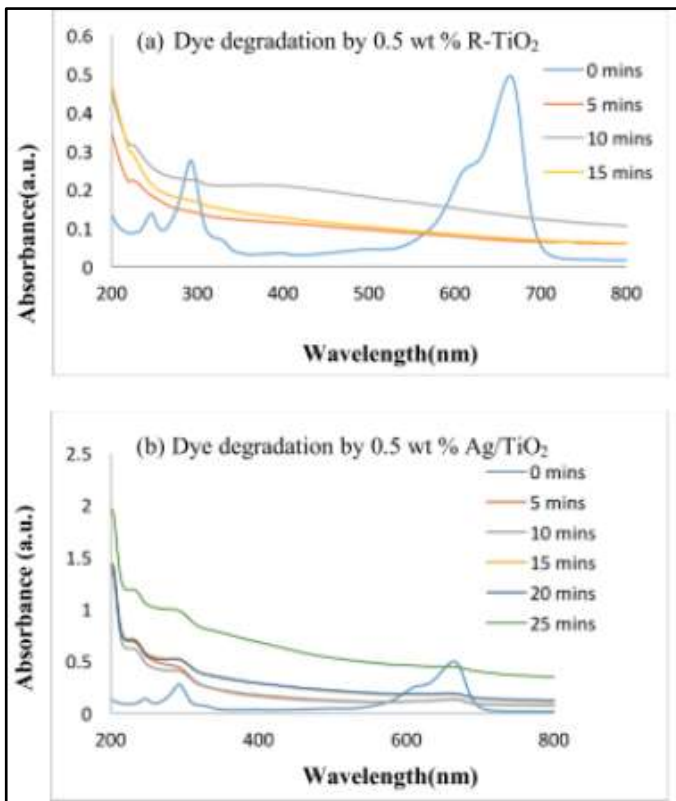


Fig. 11. Degradation of dye by (a) 0.5 wt % $Ag/R-TiO_2$ and (b) 0.5 wt % Ag/TiO_2 in sunlight.

Catalysts	Light Irradiation	Time (mins)	% Degraded
Bare TiO_2	visible	45	35 %
1 wt % $Ag/R-TiO_2$	visible	30	100 %
Ag/TiO_{2cryst}	visible	30	74 %
Ag/TiO_2	visible	30	80 %
0.5 wt % $Ag/R-TiO_2$	visible	25	100 %
Ag/TiO_{2cryst}	visible	25	72 %
Ag/TiO_2	visible	25	72 %
0.2 wt % $Ag/R-TiO_2$	visible	25	74 %
Ag/TiO_{2cryst}	visible	25	74 %
Ag/TiO_2	visible	25	7 %
0.5 wt % $Ag/R-TiO_2$	Sunlight	5	100 %
0.5 wt % Ag/TiO_2	Sunlight	25	100 %

Table 2. Photodegradation of MB by different catalysts.

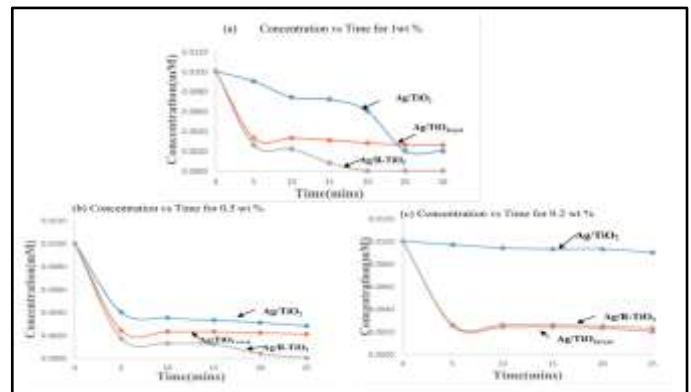


Fig. 12. Photocatalytic efficiency of different silver loaded catalysts.

IV. CONCLUSION

Anatase and Rutile phases of titanium dioxide nanoparticles namely TiO_2 , TiO_{2cryst} and $R-TiO_2$ were employed in their bare as well and silver loaded TiO_2 nanoparticles for the degradation of MB. The Bare TiO_2 nanoparticles did not degrade the dye while the metal loaded form actively degraded the dye which was also dependent upon the percentages of metal loaded upon it. Out of the three forms taken $Ag/R-TiO_2$ was most photocatalytically active in degradation of dye under visible and sunlight irradiation which further was dependent on different weight percentages of metal loaded over it (0.2 wt %, 0.5 wt %, 1 wt %). 0.5 wt % $Ag/R-TiO_2$ effectively degraded the dye in 25 minutes under visible light irradiation. Even 1 wt % $Ag/R-TiO_2$ showed the complete removal of MB in just 5 minutes.

V. ACKNOWLEDGEMENT

My sincere respect and heartfelt acknowledgement to Dr. Jaspreet Kaur for her relentless support and unwavering contribution in the building of this work. I am also grateful to the faculty members and supporting staff, School of Basic Sciences and Research and School of Engineering and



Technology, Sharda University, Greater Noida for their unconditional support, encouragement and way forward. In particular, my sincere acknowledgement to Dr. Viney Kumar Verma and Dr. Geeta Durga for their invaluable advice and guidance. I would also like to thank PhD Scholars in Material Research Lab for rendering their help.

23. Maicu, M. Hidalgo, Colon M.C., Navio G., J.A.J. *Photochem. Photobiol A*, 217 (2011) 275–283.
24. Han, F. Kambala, Srinivasan V. S. R., Rajarathnam M., Naidu D., (2009) *R. Appl. Catal, A: Gen.* 359 25–40.

VI. REFERENCES

1. Kumar S. G., J. (2011) *Phys. Chem.*, 115A 13211–13241.
2. Kamat P. V., (1993) *Chem. Rev*, 93 267-300.
3. Gratzel A. M., (1995) *Chem. Rev*, 95 49-68
4. Fujishima A, Rao T. N., Tryk D. A., J. (2000) *Photochem. Photobio. C: Photochem. Rev.* 1 1–21.
5. Fox M. A. , Dulay M. (1993) *Chem. Rev.* 93 341-357.
6. A. D. Paola, Bellardita, L.Palmisano, *catal rev*, 3 (2013) 36-73
7. G. S. Mital, T. Manoj, *Chinese sci bull*, 56 (2011) 16
8. Hu C, Lan Y, Qu J., Hu X., Wang A., (2006) *Environ. Sci. Technol*, 110 4066-4072 .
9. Linsenbigler A. L., G. Lu, Yates J. T., (1995) *Chem. Rev.* 95 735-758.
10. Chen X., Mao S. S., (2007) *Chem. Rev*, 107, 2891-2959.
11. Thiruvenkatachari R. Vigneswaran S., Moon S., (2008) *Korean J. Chem. Eng*, 25 64-72.
12. Mills A., Hunte S. L., (1997) *J. Photochem. Photobio A: Chem*, 108 1-35.
13. Kudo A., Miseki Y., (2009) *Chem. Soc. Rev*, 38 253–278.
14. Yang P, Lu C, Hua N, (2002) *Mater Lett*, 57, 794–801.
15. Song K., Zhao J, Bao J, (2008) *J Am Ceram Soc*, 91 1369-1371
16. Lachheb H., Puzenat E., Houas A., Ksibi M., Elaloui E., Guillard C., Herrmann J.M. (2002) 39 75–90.
17. Hidalgo M.C., Maicu M., Navio J.A., Colon G., (2007) *Catal. Today* 129 43.
18. Yogi C., Kojima K., Hashishin T., Wada N., Inada Y., Gaspera E.D., Bersani M., Martucci, L. Liu, Sham T.K., (2011) *J. Phys. Chem. C* 115 6554.
19. Zainab N. Jameel, Dr. Adawiya J. Haider, Dr. Samar Y. Taha. (2014) *Eng & Tech*, 32 , 3
20. Aysin Basak, Park Jongee, Ozturk Abdullah. *Nanocon*, (2011) 9 21 – 23
21. Muneer M. BaAbbad, Abdul Amir H. Kadhun, Abu Bakar Mohamad, Mohd S. Takriff, Kamaruzzaman Sopian. (2012) *Int. J. Electrochem. Sci.*, 74871 - 4888
22. Kuvarega Alex T., Rui W. Krause M., Bhokie B. Mamba (2011) . *Phys. Chem. C*, 115 22110–22120